Sakarya University Journal of Science

ISSN : 2147-835X
Publisher : Sakarya University

Vol. 28, No. 6, 1326-1341, 2024
DOI: https://doi.org/10.16984/saufenbilder.1469172

Research Article

Finite Element Modeling of RC Beams Produced with Low-Strength Concrete and Strengthened for Bending and Shear with CFRP and GFRP

Ali Sarıbıyık, Yusuf Sümer*, Wael Mansur Aldbahir

Sakarya University of Applied Sciences, Faculty of Technology, Department of Civil Engineering, Sakarya, Türkiye, alisaribiyik@subu.edu.tr, ysumer@subu.edu.tr, d190007004@subu.edu.tr

ARTICLE INFO

Keywords:
Reinforced concrete beam
Strengthening
Finite element model
CFRP, GFRP

Article History:
Received: 18.04.2024
Accepted: 17.12.2024
Online Available: 28.12.2024

ABSTRACT

In this study, the analysis of reinforced concrete (RC) beams strengthened with Fiber Reinforced Polymer (FRP) composites against bending and shear loads was carried out with the finite element technique, using ABAQUS software, which is widely used in simulating experimental circumstances in numerical studies. It has been reported that buildings in areas damaged by earthquakes are generally constructed using low-strength concrete and inadequate reinforcement. Additionally, construction errors also contribute to reducing the load-bearing capacity of structural elements. For this purpose, nine rectangular cross-section RC beams were experimentally constructed using low-strength concrete and inadequate bending and shear reinforcement. These beams were strengthened by wrapping them in different configurations with Carbon and Glass FRP (CFRP and GFRP) composites to resist shear and bending forces in both transverse and longitudinal directions, and their load-displacement curves were obtained. Subsequently, a three-dimensional Finite Element Model (FEM) was created to validate the experimental results. The FEM validation demonstrated high accuracy in replicating experimental outcomes, emphasizing the influence of mesh size, dilation angle, and concrete constitutive models on simulation fidelity. Parametric studies revealed that increasing longitudinal reinforcement diameters had minimal effect on load capacity but highlighted the critical role of transverse reinforcement, as reducing stirrup spacing significantly improved load-bearing capacity. GFRP-reinforced beams exhibited superior ductility and a 15% higher strength compared to CFRP, suggesting their suitability for applications demanding enhanced displacement capacity. Furthermore, the findings underline the need for refined FEM models to better capture inclined fiber orientations and optimize structural reinforcement strategies.

1. Introduction

When assessing the aftermath of earthquakes, extensive research has revealed that the accelerated and unregulated construction practices resulting from population growth have led to substantial shortcomings in the implementation of RC building techniques. Numerous investigations have indicated that deficiencies in reinforcement, substandard material quality, and, notably, errors in craftsmanship and application, have had a deleterious impact on the seismic resilience of structures, resulting in significant human and property losses [1-6]. Consequently, the expeditious and cost-effective retrofitting of structural elements within seismically deficient buildings assumes paramount importance.

In recent years, there has been a significant emphasis on reinforcing RC elements through the utilization of carbon and glass reinforced polymer materials, owing to notable advancements in construction materials technologies. These materials are distinguished by their exceptional attributes, including their lightweight nature, high tensile strength, ease of application, and corrosion resistance, thereby

Cite as: A. Sarıbıyık, Y. Sümer, W. M. Aldbahir (2024). Finite Element Modeling of RC Beams Produced with Low-Strength Concrete and Strengthened for Bending and Shear with CFRP and GFRP, *Sakarya University Journal of Science*, 28(6), 1326-1341. https://doi.org/10.16984/saufenbilder.1469172

establishing them as viable alternatives for traditional reinforcement materials. Specifically, in the context of beam strengthening, the practice of employing carbon and glass fiber polymers has gained prominence.

This technique involves the external wrapping of beams in various configurations to enhance their structural integrity without necessitating an increase in the beam's cross-sectional dimensions, thereby averting potential structural overload [7-18]. Numerous experimental and numerical studies have consistently indicated that these reinforcement methods significantly enhance the flexural and shear strength of RC elements [19-26]. Nonetheless, it is evident that additional research endeavors are indispensable to ascertain the requisite parameters for achieving optimal strengthening outcomes.

In recent years, the advancement of computer technologies has significantly accelerated and enhanced the execution of experimental studies within a computerized environment, facilitated by the utilization of numerical calculation methods. Among these methods, Finite Element Analysis (FEA) stands out as a prominent numerical technique employed to address analytically insurmountable or intricate engineering problems. FEA finds extensive application across various engineering domains, including civil engineering, mechanical engineering, and aerospace engineering. The successful application of the finite element method hinges on the initial step of accurately defining material properties and behavioral models in the most realistic manner possible.

ABAQUS is a widely employed FEA software package for addressing both linear and nonlinear engineering problems. To gain insights into and analyze the structural behavior of beams with varying properties under different loading conditions, experimental investigations can be effectively conducted through the utilization of the ABAQUS program [27-32]. An essential consideration in this context is the necessity to validate the FEM constructed with experimental studies available in the existing literature. This verification process enables the subsequent execution of parametric studies on well-established models.

This study presents the experimental findings pertaining to the enhancement of weakly strengthened RC beams against shear and bending using Fiber-Reinforced Polymer (FRP) composites. Subsequently, the load-displacement curves of these beams are corroborated through FEM analysis. The research proceeds to conduct sensitivity analyses concerning the material models and behavior models employed for the beam specimens, identifying and elaborating on the recommended FEM parameters. Furthermore, the investigation delves into assessing the impact of utilizing longitudinal and transverse reinforcement on the behavior of beams reinforced with Carbon Fiber Reinforced Polymer (CFRP) and Glass Fiber Reinforced Polymer (GFRP) through a parametric study.

2. Experimental Study

The outcomes of the experimental investigation incorporated into the FEM originate from a thesis dedicated to the reinforcement of RC beams characterized by diminished flexural and shear strength and low concrete strength. This reinforcement was achieved through the application of Fiber-Reinforced Polymer (FRP) composites, as documented in reference [19]. Using unidirectional FRP textiles, the reinforced beams were wrapped as U-shape design to increase their resistance to shear and bending stresses. Subsequently, these beams were subjected to four-point bending tests.

The test configuration comprised a set of one control beam and eight reinforced beams. The beams shared a common loading span of 600mm, and the stirrup spacing was consistently designed to be fixed at 150mm. In this context, the beam strength results obtained from the experimental study are presented alongside the corresponding outcomes from the finite element modeling analysis.

2.1. Properties of test beams

The cross-sectional details, reinforcement specifications, and loading characteristics of the RC beams manufactured in the experimental investigation are illustrated in Figure 1. These beams possess a cross-sectional dimension of

150×250 mm and a span length of 1800mm. The ratio of shear span to the effective height is 2.65 for beams featuring Ø10 reinforcement in both the tension and compression zones. Table 1 provides a list of abbreviated names and reinforcement types for the RC beams, for which bearing capacities and deflection behaviors were assessed through a four-point bending test.

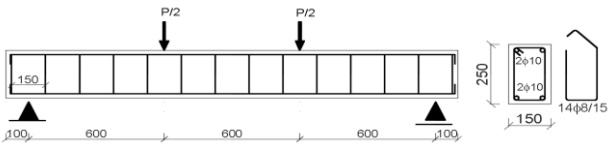

Figure 1. RC beam loading case and geometric properties

Table 1. Beam specimen coding and descriptions

Beam name	Beam shapes	Beam properties
Control Beam (C.B)		-
CFRP11		one layer longitudinal, one layer 90° transverse wrapped with CFRP
CFRP22		Two layers longitudinal, two layers 90° transverse wrapped with CFRP
CFRP21-1		Two layers longitudinal, one layer 90° transverse, one layer 45° transverse wrapped with CFRP
GFRP11		One layer longitudinal, one layer 90° transverse wrapped with GFRP
GFRP21		Two layers longitudinal, one layer 90° transverse wrapped with GFRP
GFRP22		Two layers longitudinal, two layers 90° transverse wrapped with GFRP
GFRP21-1		Two layers longitudinal, one layer 90° transverse, one layer 45° transverse wrapped with GFRP
GFRP20		Two layers longitudinally wrapped with GFRP

2.2. Properties of materials

The concrete employed in the RC beam specimens exhibited an average compressive strength, strain capacity, and modulus of elasticity of 17.13 MPa, 0.0025, and 194.50 GPa, respectively[19]. The longitudinal reinforcement utilized in the beams possessed yield and tensile strengths of 479 MPa and 599 MPa, respectively. Meanwhile, the stirrup reinforcement exhibited yield and tensile strengths of 368 MPa and 525 MPa, respectively. To strengthen the beams,

unidirectional Glass and Carbon fiber fabrics were employed. The properties of the reinforcement materials used are detailed in Table 2.

Table 2. Materials used and their properties

Material properties	Carbon fiber fabric	Glass fiber fabric	Epoxy Resin
Density (g/cm^3)	1.79	2.56	1.31
Tensile strength (MPa)	3900	2300	30
Tensile elastic modulus (GPa)	230	76	4.50
Weaving thickness (mm)	0.17	0.166	-

3. Finite Element Model Parameters

Three-dimensional finite element models were constructed for RC beam specimens reinforced with CFRP and GFRP composites, taking into account the boundary conditions and loading conditions applied during the experiments. The "Static RIKS" method was employed for beam analysis. In this method, the load magnitude is treated as an additional unknown, and both loads and displacements are solved simultaneously. Following the analysis, the loads were obtained from the supports, and the deflection was measured at a predetermined point located at the midpoint of the beam. The modeling process incorporated the "Embedded" feature, assuming an equal strain rate between the concrete and reinforcement. In this approach, the translational degrees of freedom of the embedded nodes were constrained through interpolation based on the corresponding degrees of freedom of the main element [33]. Furthermore, the "skin reinforcement" feature provided by ABAQUS was utilized to apply FRP elements in various orientations and directions on the surface of the RC beam.

This methodology allows for the definition of the mechanical properties of a different material on the surfaces of a three-dimensional element. The support conditions for the RC beams were configured to replicate those used in the experimental study, including sliding and fixed supports, as illustrated in Figure 2.

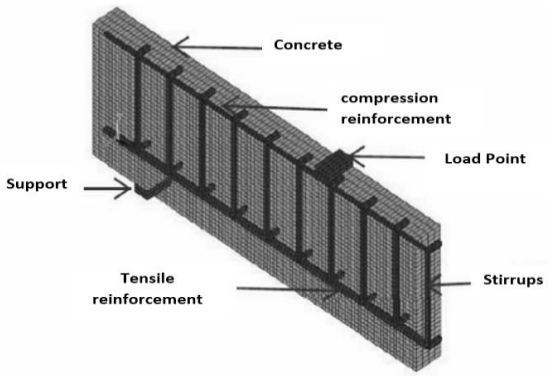

Figure 2. Finite element model symmetrical view

In the finite element definitions, the solid C3D8R element with 8 nodes and reduced integration feature from the ABAQUS material library was employed for modeling concrete. In the case of FRP elements, the S4R element, compatible with shell modeling, was selected. The S4R element is a 4-node quadrilateral shell element incorporating a reduced integration and a large strain formulation, as depicted in Figure 3. The utilization of reduced integration elements, which employ fewer integration points compared to full integration elements, serves to decrease computational analysis time. For the representation of reinforcement bars, a two-node linear truss element (T3D2), well-suited for three-dimensional modeling, was utilized.

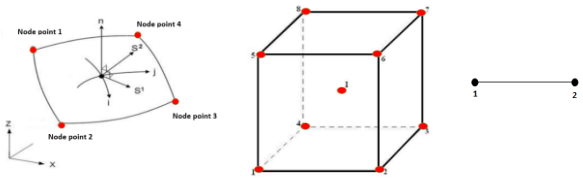

a) S4R shell element b) C3D8R solid element c)T3D2 bar element

Figure 3. Finite elements types

3.1. Concrete material model

In order to simulate the cracking, softening, and progressive degradation of concrete under various loading conditions, the Concrete Damage Plasticity (CDP) model combines the ideas of plasticity and damage were used for modeling the concrete. This model enables researchers to predict the complex behavior of concrete more accurately and provide more precise results under different conditions. In the CDP model, crack initiation is postulated to occur at locations

where the maximum principal strain is positive. Plasticity, in this context, refers to deformation that remains irreversible even after all external loads are removed [34, 35].

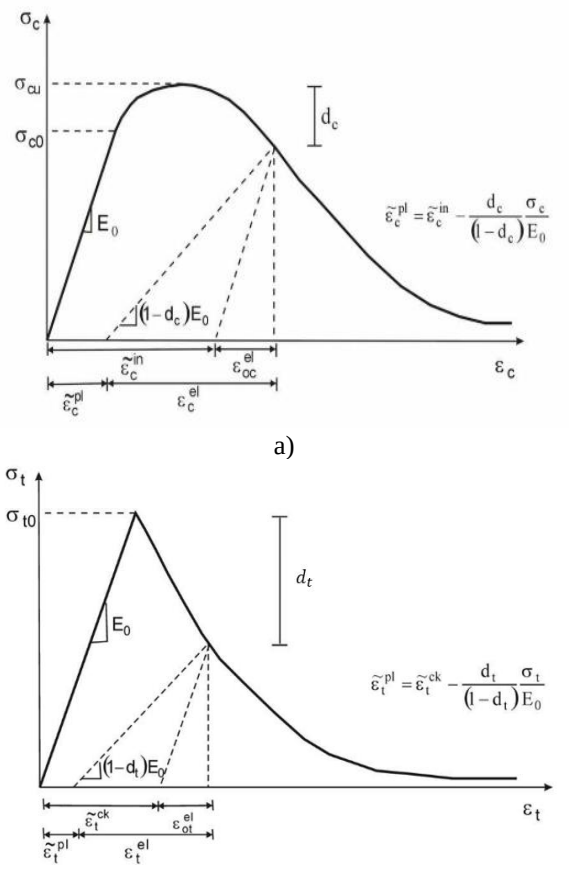

a)

b)

Figure 4. Concrete behavior under a) compression b) and axial tension [36]

Damage, typically identified by a reduction in the elastic modulus, is primarily attributed to two principal failure mechanisms within the CDP framework: tensile cracking and compressive crushing of concrete. The stress-strain relationships under uniaxial tension and compression, as illustrated in Figure 4, are determined through equations 1-5 [36].

In these equations, E_0 signifies the initial (undamaged) elastic modulus of the material, while $\varepsilon_c^{\sim pl}$, $\varepsilon_c^{\sim in}$, $\varepsilon_t^{\sim pl}$,, and $\varepsilon_t^{\sim ck}$ represent the plastic strain in compression, inelastic strain under compression, plastic strain in tension, and plastic strain under tension, respectively.

The computation of compressive and tensile damage variables, denoted as d_c and d_t, respectively, is achieved using equations 6-7 [37]. Within these equations, the parameters b_t and b_c symbolize the relationship between plastic and inelastic deformations, and they are presumed to be 0.7 within the analysis.

$$\varepsilon_c^{in} = \varepsilon_c - \frac{\sigma_c}{E_0} \text{ and } \varepsilon_t^{ck} = \varepsilon_t - \frac{\sigma_t}{E_0} \quad (1)$$

$$\varepsilon_c^{\sim pl} = \varepsilon_c^{\sim in} - \frac{d_c}{(1-d_c)} \cdot \frac{\sigma_c}{E_0} \quad (2)$$

$$\varepsilon_t^{\sim pl} = \varepsilon_t^{\sim ck} - \frac{d_t}{(1-d_t)} \cdot \frac{\sigma_t}{E_0} \quad (3)$$

$$\sigma_c = (1-d_c) \cdot E_0 \left(\varepsilon_c - -\varepsilon_c^{\sim pl}\right) \quad (4)$$

$$\sigma_t = (1-d_t) \cdot E_0 \left(\varepsilon_t - -\varepsilon_t^{\sim pl}\right) \quad (5)$$

$$d_c = 1 - \frac{\sigma_c \cdot E_o^{-1}}{\sigma_c \cdot E_o^{-1} + \varepsilon_c^{in}(1-b_c)} \quad (6)$$

$$d_t = 1 - \frac{\sigma_t \cdot E_o^{-1}}{\sigma_t \cdot E_o^{-1} + \varepsilon_t^{ck}(1-b_t)} \quad (7)$$

In the literature, numerous tension stiffening models have been proposed to depict the tensile-softening behavior of concrete beyond its maximum tensile strength.

In this study, the tensile stress-strain curve was established using the approach outlined by Genikomsou and Polak in 2015 [38], as illustrated in Figure 5. The calculation of the fracture energy (G_f) is conducted following equations 8-9 [39]. For normal weight concrete, the G_f parameter, as specified in CEB-FIB 2010 [39], is computed as follows:

$$G_f = 0.073 f_{cm}^{0.18} \quad (8)$$

$$f_{cm} = f_{ck} + \Delta f \quad (9)$$

In these equations, f_{cm} is the average compressive strength (MPa) and Δf is taken as a constant of 8 MPa. The stress-strain curves obtained from concrete models developed by Mander, Kent Park, and Hognestad [40] were employed to simulate the compressive behavior of the

concrete, which was essential for the FEM (Figure 5). In the process of validation of the experimental results, these models were compared to ascertain the most suitable behavior model.

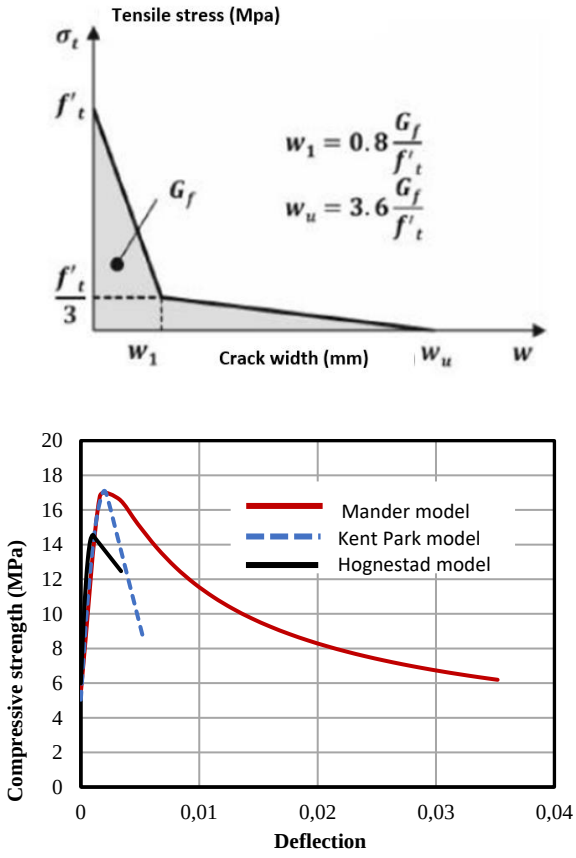

Figure 5. The models for the decrease in tensile stress [38] and the concrete behavior models.

3.2. Reinforcing steel model

In the modeling process, the material model for steel reinforcement is characterized as elasto-plastic, described by equations 10-12. This model is based on the consolidation behavior outlined in the Turkish Earthquake Code [41], and the stress-strain curve for this model is presented in Figure 6. Within this context, the parameters are defined as follows: f_{sy} represents the steel yield strength, f_{su} denotes the steel rupture strength, ε_{sy} signifies the steel yield strain, ε_{su} represents the steel rupture strain, ε_{sh} indicates the steel consolidation strain, and E_s signifies the steel modulus of elasticity.

$$f_s = E_s\,\varepsilon_s, \qquad \varepsilon_s \le \varepsilon_{sy} \tag{10}$$

$$f_s = f_{sy}, \qquad \varepsilon_{sy} < \varepsilon_s \le \varepsilon_{sh} \tag{11}$$

$$f_s = f_{su} - (f_{su} - f_{sy})\frac{(\varepsilon_{su} - \varepsilon_s)^2}{(\varepsilon_{su} - \varepsilon_{sh})^2}, \qquad \varepsilon_{sh} < \varepsilon_s \le \varepsilon_{su} \tag{12}$$

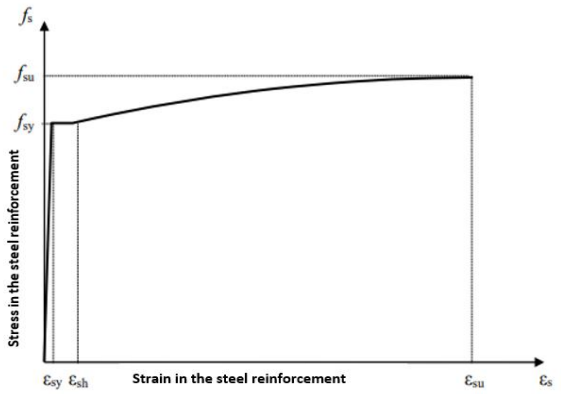

Figure 6. Reinforcement stress-strain model [41]

3.3. FRP material model

The "skin-reinforcement" feature was employed to delineate CFRP or GFRP elements on both the underside and lateral surfaces of the beam, as depicted in Figure 7a.

$$f_f = E_f \varepsilon_f \qquad \varepsilon_f \le \varepsilon_{fu} \tag{13}$$

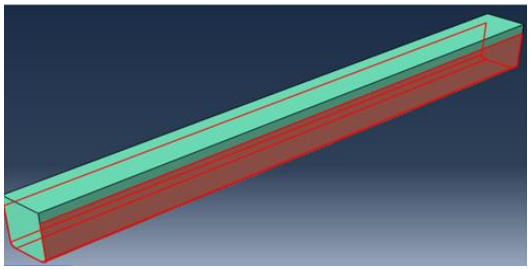

a)

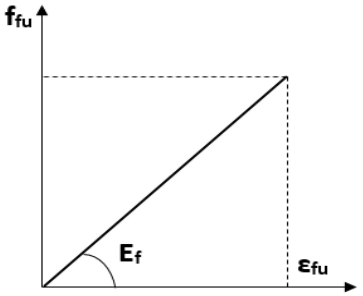

b)

Figure 7. a) Element skin used to simulate FRP, b) FRP material model

It's worth noting that FRP material is characterized as a linear elastic substance devoid of plastic behavior. The stress-strain relationship for FRP is considered to be linear elastic until the point of rupture, as illustrated in Figure 7b and articulated in the equation 13. Given the brittle

nature of FRP, the "Lamina" behavior model was implemented in the modeling process. The relevant parameters utilized in the modeling can be found in Figure 8. In the equation, f_{fu} and ε_{fu} represent the maximum failure stress and strain of FRP at failure, respectively, and E_f represents the Modulus of Elasticity of FRP.

CFRP Strengthening material

E1	E2	Nu12	G12	G13	G23
230000	4500	0.1	0.1	0.1	0.1

Ten Stress Fiber Dir	Com Stress Fiber Dir	Ten Stress Transv Dir	Com Stress Transv Dir	Shear Strength	Cross-Prod Term Coeff	Stress Limit
3900	0.1	30	0.1	0.1	0.1	3900

GFRP Strengthening material

E1	E2	Nu12	G12	G13	G23
76000	4500	0.1	0.1	0.1	0.1

Ten Stress Fiber Dir	Com Stress Fiber Dir	Ten Stress Transv Dir	Com Stress Transv Dir	Shear Strength	Cross-Prod Term Coeff	Stress Limit
2300	0.1	30	0.1	0.1	0.1	2300

Figure 8. FRP material properties

3.4. Finite element mesh properties

In the process of generating finite element meshes, three distinct solution meshes, as depicted in Figure 9, were employed. The parametric investigation was subsequently pursued using the solution mesh that yielded the most favorable outcome.

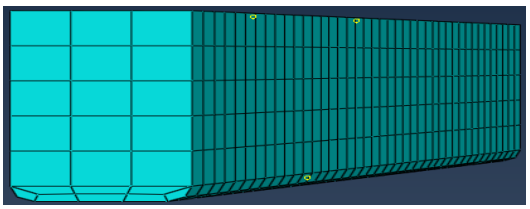

Mesh type : Hex

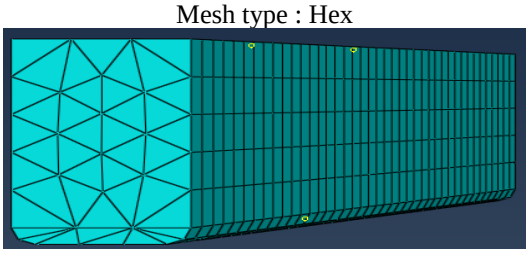

Mesh type: Wedge

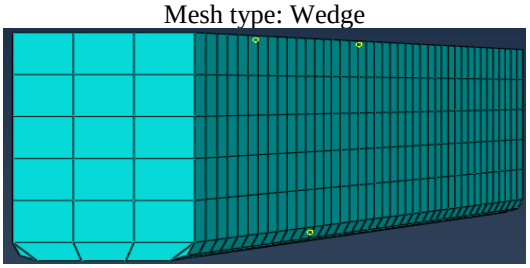

Mesh type: Hex-Dominated

Figure 9. Mesh creation of beams

4. Finite Element Analysis Results

4.1. Control beam verification results

Utilizing the developed finite element model, experimental validations were conducted, employing the material models detailed in the preceding section. To establish the strength depletion envelope within the CDP method, four fundamental parameters were defined.

These parameters include the dilation angle, the eccentricity parameter (ϵ), the ratio of the initial axial compressive yield stress under biaxial loading to the initial axial compressive yield stress (σ_{bo}/σ_{co}), and the ratio of the stress on the tensile meridian at the initial yield point to the compressive stress (K_c). Among these parameters, eccentricity (ϵ), σbo/σco, and K_c were initially set as default values of 0.1, 1.10, and $2/3$, respectively.

The dilation angle was subsequently determined based on the analysis outcomes. In the modeling process, the loading was applied to the top surface of the beam as a structural singular load, mirroring the experimental setup. Following the analysis, the loads were extracted from the supports, and the deflection was measured at the midpoint of the beam. Upon scrutinizing the results, it becomes evident that among the concrete behavior models, the Mander model yields the most favorable outcome (Figure 10a). However, it was observed that alterations in the solution mesh had a limited impact on the results. In this context, it was ascertained that the $50\ mm$ solution mesh, among the closely spaced meshes employed, sufficiently approximated the experimental results (Figure 10b). Additionally, the various solution mesh generation methods that were comparably close, with the Hexagonal-dominated method demonstrating the most favorable outcome (Figure 10c). Regarding the analysis of the dilation angle, which is a pivotal parameter in modeling, it was established that a dilation angle of 40 degrees sufficed for validation purposes, aligning with findings in the literature [42, 43] (Figure 10d).

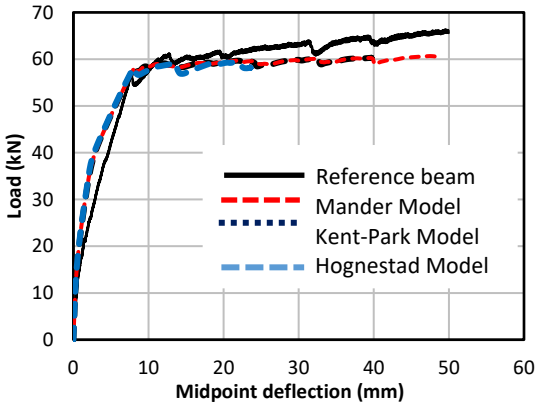

a)

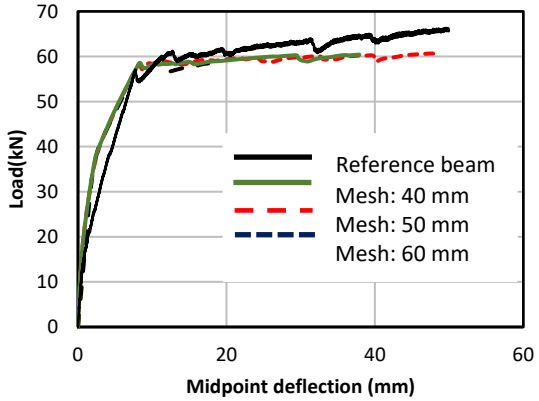

b)

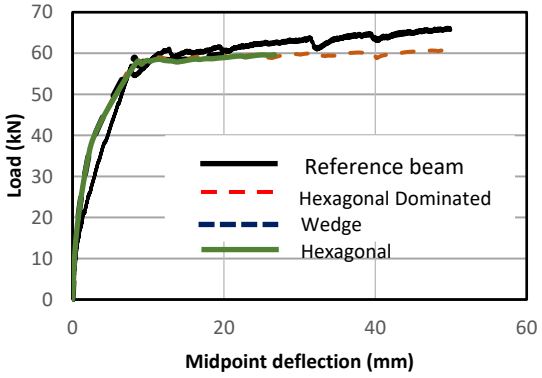

c)

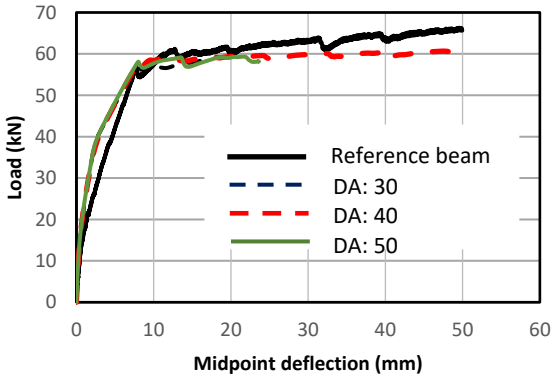

d)

Figure 10. Experiment validation results a) Result according to concrete models, b) Generated mesh results, c) Different mesh model results, d) Results of dilation angles (DA)

Upon investigating the occurrence of crack formation, it was observed that the FEM accurately represented the cracks extending up to the top of the neutral axis under maximum bending, consistent with the experimental findings (Figure 11). This alignment between the model and experiment indicates a high level of compatibility.

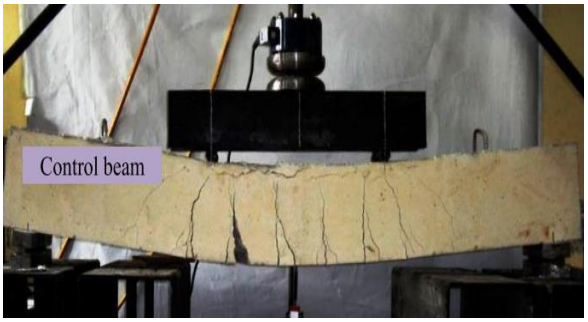

a) Crack formation in the test beam

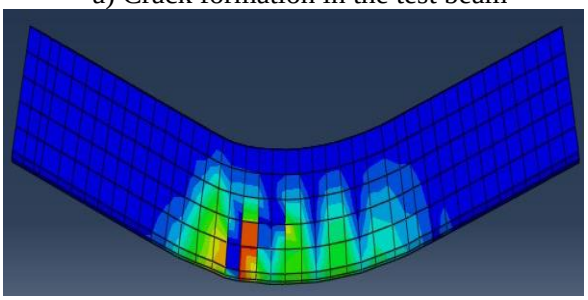

b) Crack formation of FEM

Figure 11. Comparison of crack formations

4.2. Reinforced beam validation results

The outcomes of the RC beams strengthened with FRP materials are presented in Table 3. Upon comparing the results, particularly in terms of maximum load and displacement, it becomes evident that there is a significant alignment between the outcomes.

Table 3. Analysis results of strengthened beams

Beam ID	Max. Load Pu (kN)		$\frac{Pu,Exp.}{Pu,FEM}$	Deflection $\delta_u(mm)$		$\frac{\delta_u,Exp.}{\delta_u,FEM}$
	Exp.	FEM		Exp.	FEM	
CFRP11	168.77	168.8	***0.99***	34.54	32.74	***1.05***
CFRP22	171.8	166.6	***1.03***	23.81	22.36	***1.06***
CFRP21-1	167.6	181.5	***0.92***	25.1	30.4	***0.83***
GFRP11	121.2	122.9	***0.99***	34.9	36.1	***0.97***
GFRP22	159.1	161.3	***0.98***	36.1	37.8	***0.96***
GFRP21	146.9	148.5	***0.99***	32.3	34.7	***0.93***
GFRP21-1	161.9	190.3	***0.85***	31.6	46.6	***0.68***
GFRP20	132.4	131.2	***0.99***	29.3	29.1	***1.00***

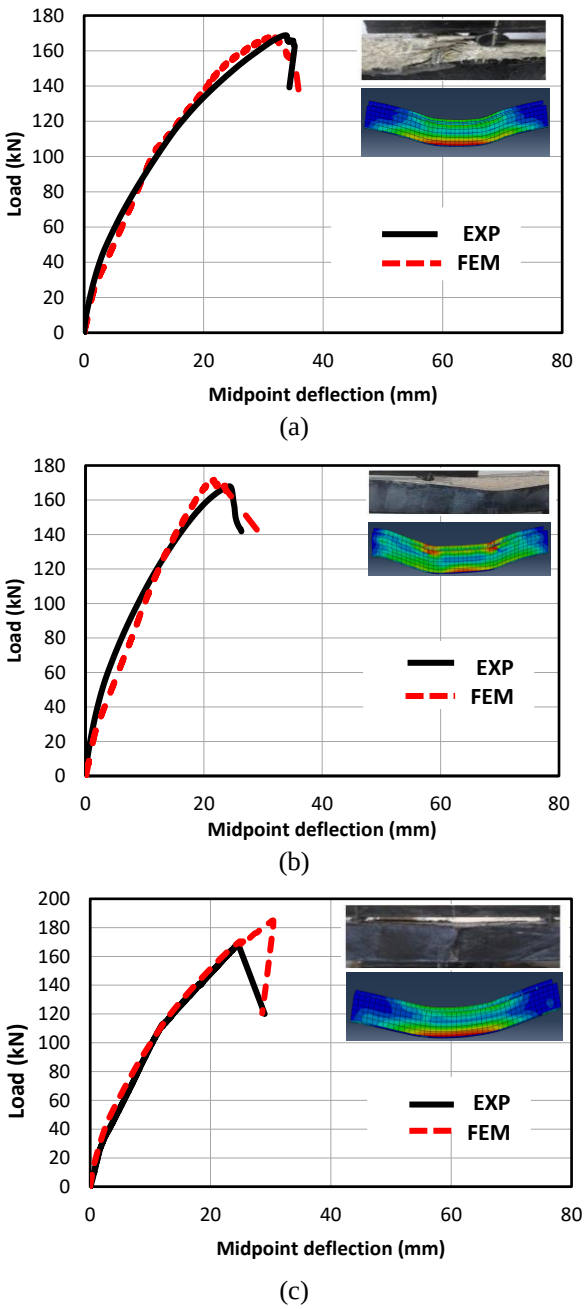

Figure 12. Experimental and FEM results of CFRP reinforced beams (a) CFRP11, b) CFRP22, c) CFRP21-1

This implies that the proposed finite element model is capable of accurately simulating the results with a satisfactory level of accuracy. However, it should be noted that as the degree of transverse wrapping increases, there is some divergence in the results.

When comparing the test results of the beams reinforced with CFRP composites using various methods with the FEM analysis outcomes, it was observed that the load-deflection curves exhibited a high degree of consistency (Figure 12).

Specifically, the load and deflection results for the CFRP11-strengthened beam were confirmed with a match of 99%, while for the CFRP22 and CFRP21-1 strengthened beams, the results for load and deflection were confirmed at 97%, 94%, 92%, and 83%, respectively as represented in Figure 12.

Upon analyzing the results of the analysis for beams reinforced with GFRP and CFRP composites in various configurations, it is evident that the load-deflection curves demonstrate acceptable proximity (Figure 12-13).

Upon closer examination of the load and deflection results, it can be observed that they are confirmed at a rate of 99%, 97%, 98%, and 96% for the beam reinforced with GFRP11 (one layer longitudinally and one layer 90° transversely wrapped) and GFRP22 (two layers longitudinally and two layers 90° transversely wrapped) (Figure 13a-b).

For beams reinforced with GFRP21 (two layers longitudinally and one layer 90° transversely wrapped), the results were confirmed at 99% and 93%, respectively (Figure 13c). However, it is notable that the load-displacement values are simulated with a degree of accuracy ranging from 85% to 68% for beams reinforced with GFRP21-1 and GFRP20 (two layers longitudinally wrapped), while achieving a higher level of accuracy at 99% (Figure 13d-e).

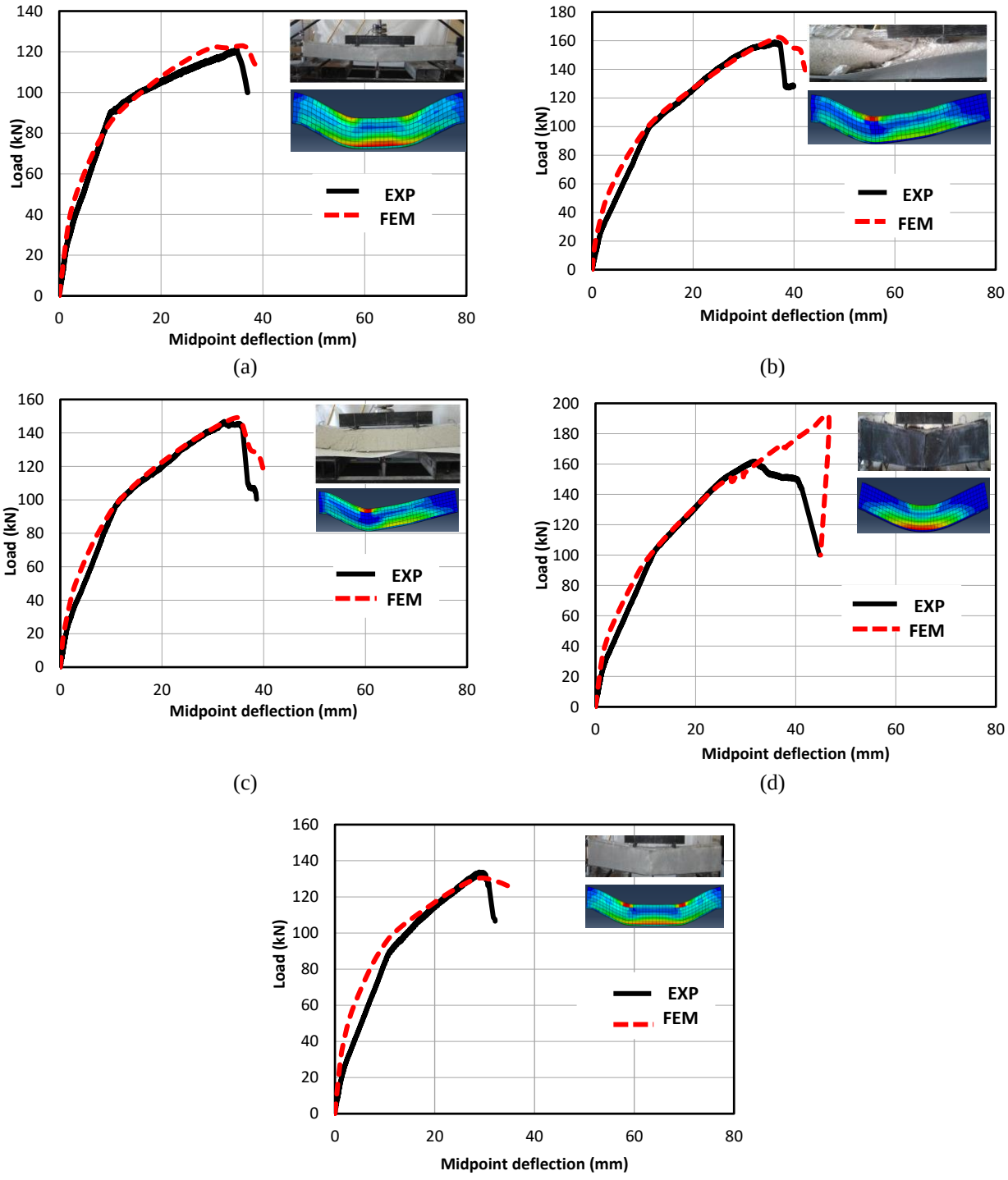

Figure 13. Test and FEM analysis results of GFRP reinforced beams (a) GFRP11, b) GFRP22, c) GFRP21, d) GFRP21-1, e) GFRP20)

5. Parametric Study

In this section, a parametric study was conducted to examine the impact of varying certain parameters on the strength of the beams, which were not considered in the experimental investigation. The experimental study utilized a single type of longitudinal reinforcement (2Ø10), with a stirrup spacing designated as Ø8/15. Consequently, the parametric study aimed to explore the influence of different reinforcement configurations on the behavior of CFRP and GFRP reinforced beams, as outlined in the subsequent sections.

5.1. Effect of longitudinal reinforcement diameter and stirrup on behavior

To assess the impact of longitudinal reinforcement and stirrups on the reinforced beams, analyses were conducted with reference to CFRP11 and GFRP11 beams. The nomenclature for the newly analyzed beams is presented in Table 4. The study encompassed four distinct longitudinal reinforcement diameters and three varying stirrup spacing configurations. In the numerical investigation, FEM analyses were conducted on CFRP11 and CFRP22 reinforced beams while modifying the diameters of longitudinal reinforcement, maintaining a $15\,cm$ stirrup spacing. Subsequently, additional models were analyzed by varying the stirrup spacing on a beam with constant longitudinal reinforcement. The graphs resulting from the FEA of RC beams reinforced with CFRP and GFRP, utilizing the ABAQUS program, are depicted in Figure 14. It is evident that as the diameter of longitudinal reinforcement increases in CFRP-reinforced beams, ductility decreases.

Table 4. Nomenclature of analysis beams

Sample name	Description
CFRP11-2Ø10-SØ8/15	One layer longitudinal + one layer transverse Carbon Fiber external reinforcement- 2Ø10 and $Ø8/15cm$ internal reinforcement
GFRP11-2Ø10-SØ8/15	One layer longitudinal + one layer transverse Glass Fiber external reinforcement - 2Ø10- and $Ø8/15cm$ internal reinforcement

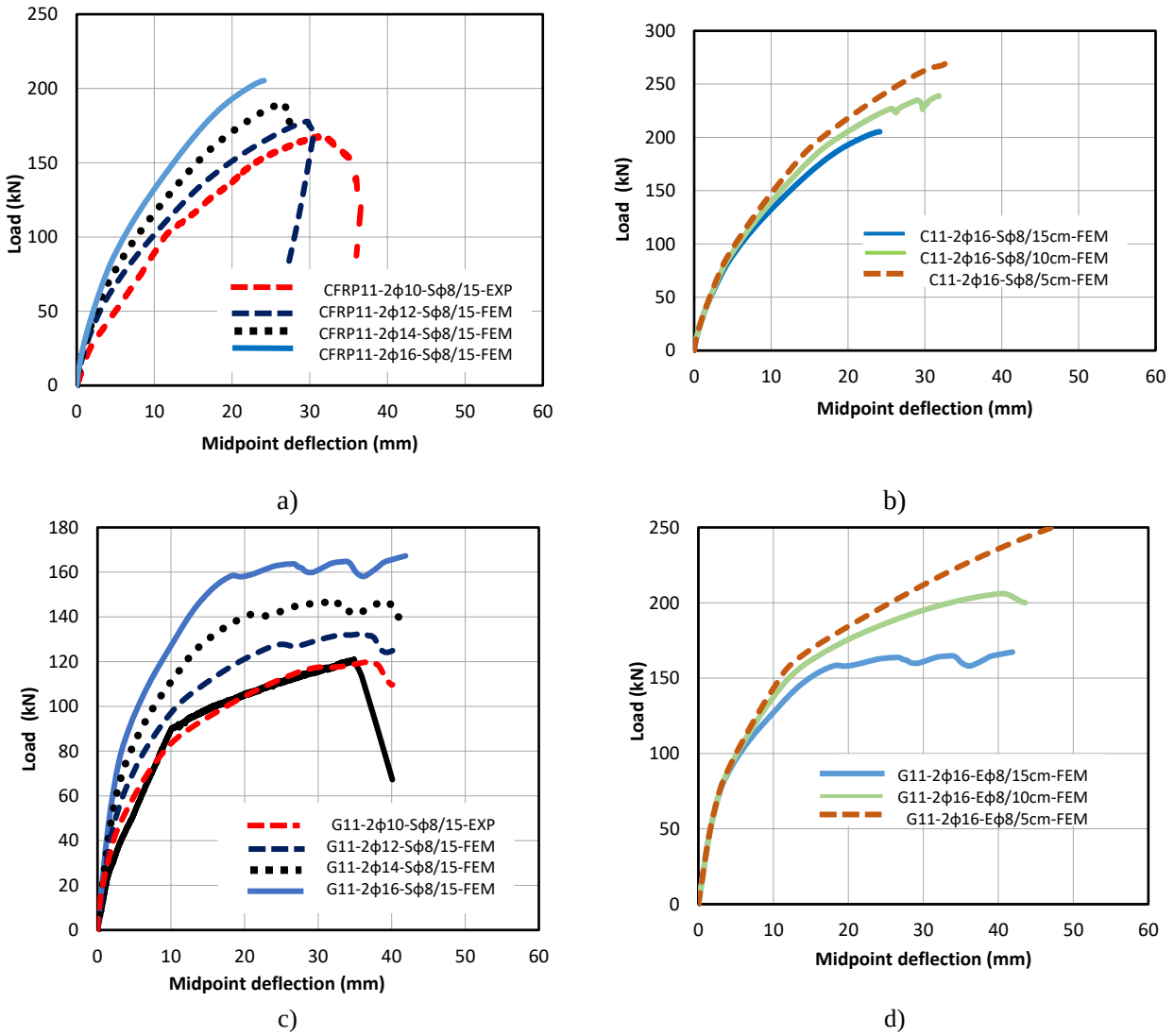

Figure 14. FEM analysis of CFRP11 beams with different reinforcement and different stirrup spacing a) Longitudinal reinforcement change in CFRP11 models, b) Stirrup spacing change in CFPR11 models, c) Longitudinal reinforcement change in GFRP11 models, d) Stirrup spacing change in GFRP11 models

Upon examining the maximum loads, there is an approximate 21% increase in the strength of the beam with Ø16 reinforcement in comparison to the beam with Ø10 reinforcement, accompanied by a 25% reduction in displacement at the midpoint (Figure 14a).

Furthermore, a decrease in stirrup spacing corresponds to an increase of roughly 60% in the displacement capacity of carbon fiber-reinforced beams, along with a 22% increase in strength (Figure 14b). Diminishing transverse reinforcement spacing yields a significant enhancement in both ductility and load-carrying capacity of the reinforced beams.

Upon analyzing the beams reinforced with glass fiber (GFRP), it becomes evident that there is an increase in ductility as the diameter of longitudinal reinforcement rises, which is contrary to the behavior observed in carbon fiber-reinforced beams. An examination of the maximum load and displacement values reveals an approximately 38% increase in the strength of the beam with Ø16 reinforcement compared to the beam with Ø10 reinforcement, accompanied by a decrease of approximately 10% in the maximum displacement value (Figure 14c).

Additionally, when the stirrup spacing is reduced, it is observed that there is a slight increase in strength and ductility in GFRP-reinforced beams, akin to the behavior observed in CFRP-reinforced beams.

A reduction in stirrup spacing from $15cm$ to $10cm$ results in approximately a 20% increase in displacement and a 25% increase in load capacity. Further decreasing the stirrup spacing from $15cm$ to $5cm$ leads to an approximately 50% increase in maximum strength (Figure 14d).

6. Conclusions and Recommendations

This study explores the analysis of rectangular section beams characterized by inadequate flexural and shear strength using the Finite Element Method. In the experimental tests, low-strength concrete and unidirectional carbon and glass fabrics were employed in beams suffering from insufficient flexural and shear reinforcement. Carbon and Glass Fiber Reinforced Polymer (CFRP and GFRP) composites were strategically oriented in both transverse and longitudinal directions, and the beams were reinforced in a U-shaped configuration.

A parametric investigation was conducted on the simulated RC beam specimen by varying solely the longitudinal and transverse reinforcements while keeping the reinforcement shapes unchanged. The ensuing results are detailed below.

- The RC control beam was accurately modeled with successful convergence using a hex-dominated solution mesh type with a mesh size of 50 mm. Additionally, a dilation angle ranging between 40 and 45 degrees was applied, and the Mander unconfined concrete model was utilized.

- When verifying the beam specimens reinforced with FRP composites, the proposed FEM produced load-displacement curves that exhibited concordance with the experimental results, achieving an accuracy of over 95% in the majority of cases. Furthermore, the model aptly simulated the experimental failure modes, thus enabling the execution of experimental studies through computer-based simulations.

- Upon analyzing the results of CFRP21-1 and GFRP21-1 specimens within the context of reinforced beam analysis, it was observed that the test results could replicate the load-displacement curves up to a specific threshold. However, the FEM model exhibited strength attainment before reaching the maximum load. Consequently, it becomes evident that the FEM model requires refinement, particularly for 45-degree inclined windings.

- It was determined that increasing the diameters of longitudinal reinforcement in the reinforced beams did not result in a significant increase in load-carrying

capacity. However, it caused shear force to become critical. In response to this, the stirrup spacing was reduced in the same model, leading to a substantial enhancement in load-carrying capacity and deflection values.

- As the diameter of longitudinal reinforcement in the beams increased, it was observed that the beams utilizing glass fiber exhibited a more ductile behavior compared to those employing carbon fiber. Nevertheless, the beams employing glass fiber achieved approximately 15% greater strength.

- Based on the outcomes of the parametric study, it was ascertained that diminishing the stirrup spacing and decreasing the diameter of longitudinal reinforcement resulted in an augmented load-bearing capacity for beams constructed with low-strength concrete. Furthermore, it was concluded that GFRP fabrics should be favored over CFRP fabrics when a higher degree of displacement capacity is desired.

Article Information Form

Funding
The author (s) has no received any financial support for the research, authorship or publication of this study.

Authors' Contribution
The authors contributed equally to the study.

The Declaration of Conflict of Interest/ Common Interest
No conflict of interest or common interest has been declared by the authors.

The Declaration of Ethics Committee Approval
This study does not require ethics committee permission or any special permission.

The Declaration of Research and Publication Ethics
The authors of the paper declare that they comply with the scientific, ethical and quotation rules of SAUJS in all processes of the paper and that they do not make any falsification on the data collected. In addition, they declare that Sakarya University Journal of Science and its editorial board have no responsibility for any ethical violations that may be encountered, and that this study has not been evaluated in any academic publication environment other than Sakarya University Journal of Science.

References

[1] N. Caglar, I. Vural, O. Kirtel, A. Saribiyik, Y. Sümer, “Structural damages observed in buildings after the 24 January 2020 Elazığ-Sivrice earthquake in Türkiye,” Case Studies in Constrtruction Materials, 2023.

[2] A. Doğangün, B. Yön, O. Onat, M. E. Öncü, S, Sağıroğlu, “Seismicity of east Anatolian of Turkey and failures of infill walls induced by major earthquakes,” Journal of Earthquake and Tsunami, 2021.

[3] B. Yön, “Identification of failure mechanisms in existing unreinforced masonry buildings in rural areas after April 4, 2019 earthquake in Turkey,” Journal of Building Engineering, vol. 43, 2021.

[4] B. Yön, O. Onat, M. E. Oncü, “Earthquake damage to nonstructural elements of reinforced concrete buildings during 2011 Van Seismic sequence,” Journal of Performance of Constructed Facilities, vol. 33, no. 6, 2019.

[5] B. Yön, E. Sayin, O. Onat, “Earthquakes and structural damages,” Earthquakes-Tectonics, Hazard and Risk Mitigation, 2017.

[6] A. Doğangün, “Performance of reinforced concrete buildings during the May 1, 2003 Bingöl Earthquake in Turkey,” Engineering Structures, vol. 26, no. 6, 2004, pp. 841–856.

[7] Y. T. Obaidat, S. Heyden, O. Dahlblom, G. Abu-Farsakh, Y. Abdel-Jawad, "Retrofitting of reinforced concrete beams using composite laminates," Construction and Building Materials, 25(2), 591-597, 2011.

[8] I. A. Sharaky, L. Torres, J. Comas, C. Barris, "Flexural response of reinforced concrete (RC) beams strengthened with near surface mounted (NSM) fibre reinforced polymer (FRP) bars," Composite Structures, 109, 8-22, 2014.

[9] S. S. Choobbor, R. A. Hawileh, A. Abu-Obeidah, J. A. Abdalla, "Performance of hybrid carbon and basalt FRP sheets in strengthening concrete beams in flexure," Composite Structures, 227, 111337, 2019.

[10] S. U. Miakhil, W. U. Shakir, G. Singh, "Retrofitting of Reinforced Concrete beams using CFRP Sheets: A Review," Strain, 70, 90, 2020.

[11] M. Panahi, S. A. Zareei, A. Izadi, "Flexural strengthening of reinforced concrete beams through externally bonded FRP sheets and near surface mounted FRP bars," Case Studies in Construction Materials, 15, e00601, 2021.

[12] R. Al-Shamayleh, H. Al-Saoud, M. Alqam, "Shear and flexural strengthening of reinforced concrete beams with variable compressive strength values using externally bonded carbon fiber plates," Results in Engineering, 14, 100427, 2022.

[13] C. Aksoylu, "Shear strengthening of reinforced concrete beams with minimum CFRP and GFRP strips using different wrapping technics without anchoring application," Steel and Composite Structures, An International Journal, 44(6), 845-865, 2022.

[14] M. E. Uz, Y. Guner, E. Avci, "Strengthening of Reinforced Concrete Beams via CFRP Orientation," Buildings, 14(1), 82, 2023.

[15] O. A. Mohamed, M. A. Kewalramani, A. M. Imran, "Shear and flexure of FRP-reinforced concrete beams and slabs–A review, Materials Today: Proceedings," 2023.

[16] K. Sengun, G. Arslan, "Performance of RC beams strengthened in flexure and shear with CFRP and GFRP," Iranian Journal of Science and Technology, Transactions of Civil Engineering, 48(1), 117-130, 2024.

[17] N. Mejía, A. Sarango, A. Espinosa, "Flexural and shear strengthening of RC beams reinforced with externally bonded CFRP laminates postfire exposure by experimental and analytical investigations," Engineering Structures, 308, 117995, 2024.

[18] J. Cui, G. Xing, P. Miao, Y. Zhang, Z. Chang, A. Q. Khan, "Flexural behavior of RC beams strengthened with BFRP bars and CFRP U-jackets: Experimental and numerical analysis," Journal of Building Engineering, 97, 110932, 2024.

[19] A. Sarıbıyık, "Beton Dayanımı Düşük Betonarme Yapı Elemanlarının Lifli Kompozitlerle Güçlendirilmesi Ve Karşılaştırılması," Sakarya Üniversitesi Fen Bilimleri Enstitüsü, 2013.

[20] C. Escrig, L. Gil, E. Bernat-Maso, F. Puigvert, "Experimental and analytical study of reinforced concrete beams shear strengthened with different types of textile-reinforced mortar," Construction and building materials, 83, 248-260, 2015.

[21] A. Siddika, M. A. Al-Mamun, R. Alyousef, Y. M. Amran, "Strengthening of reinforced concrete beams by using fiber-reinforced polymer composites: A review," Journal of Building Engineering, 25, 100798, 2019.

[22] Y. M. Alharthi, M. Emara, A. S. Elamary, I. A. Sharaky, "Flexural response and load capacity of reinforced concrete beams strengthened with reinforced mortar layer," Engineering Structures, 245, 112884, 2021.

[23] Y. J. Xue, W. W. Wang, Z. H. Wu, S. Hu, J. Tian, "Experimental study on flexural behavior of RC beams strengthened with FRP/SMA composites," Engineering Structures, 289, 116288, 2023.

[24] A. Chole, A. Tembhurne, A. Bawanthade, H. Bhadade, H. A. Khan, S. K. Shaw, "Strengthening of reinforced concrete beams by using FRPs-An overview," Materials Today: Proceedings, 2023.

[25] O. H. Hussein, A. M. Ibrahim, S. M. Abd, H. M. Najm, S. Shamim & M. M. S. Sabri, "Hybrid Effect of Steel Bars and PAN Textile Reinforcement on Ductility of One-Way Slab Subjected to Bending," Molecules, 27(16), 5208, 2022.

[26] S. M. Abd, R. Hadi, S. Abdal, S. Shamim, H. M. Najm, M. M. S. Sabri, "Effect of Using Glass Fiber Reinforced Polymer (GFRP) and Deformed Steel Bars on the Bonding Behavior of Lightweight Foamed Concrete," Buildings, 13(5), 1153, 2023.

[27] M. Aktas, Y. Sumer, "Nonlinear finite element analysis of damaged and strengthened reinforced concrete beams," Journal of Civil Engineering and Management, 20(2), 201-210, 2014.

[28] Y. Sümer, M. Aktaş, "Finite element modeling of existing cracks on pre-loaded reinforced concrete beams," Arabian Journal for Science and Engineering, 39, 2611-2619, 2014.

[29] A. Demir, N. Caglar, H. Ozturk, Y. Sumer, "Nonlinear finite element study on the improvement of shear capacity in reinforced concrete T-Section beams by an alternative diagonal shear reinforcement," Engineering Structures, vol. 120, pp. 158–165, 2016.

[30] Y. B. A. Tahnat, M. M. Dwaikat, M. A. Samaaneh, "Effect of using CFRP wraps on the strength and ductility behaviors of exterior reinforced concrete joint," Composite Structures, 201, 721-739, 2018.

[31] V. V. Cao, H. R. Ronagh, "A model for damage analysis of concrete," Advances in concrete construction, 1(2), 187, 2013.

[32] S. M. Varghese, K. Kamath, S. R. Salim, "Effect of concrete strength and tensile steel reinforcement on RC beams externally bonded with fiber reinforced polymer composites: A finite element study," Materials Today: Proceedings, 2023.

[33] Abaqus/CAE, User's Guide, V7.0, (2020). Programme, Dassault Systemes Simulia Corp. Providence, RI, USA.

[34] J. Lublineri, J. Oliver, S. Oller, E. Oñate, "A plasticdamage model for concrete," International Journal of Solids and Structures 25(3): 299–326, 1989.

[35] Y. Sumer, M. Aktas, "Defining parameters for concrete damage plasticity model," Challenge Journal of Structural Mechanics, 1(3), 149–155, 2015.

[36] Abaqus/CAE, Theory Manual, V7.0, (2020). Programme, Dassault Systemes Simulia Corp. Providence, RI, USA.

[37] A. Zangeneh Kamali, "Shear strength of reinforced concrete beams subjected to blast loading: Non-linear dynamic analysis," 2012.

[38] G. P. Balomenos, A. S. Genikomsou, M. A. Polak, M. D. Pandey, "Efficient Method for Probabilistic Finite Element Analysis with Application to Reinforced Concrete Slabs," Engineering Structures, Vol. 103, 85–101, 2015.

[39] Comité Euro-Internacional Du Béton (2010). Ceb-Fib Model Code 2010, London.

[40] V. V. Cao, and H. R. Ronagh, "A model for damage analysis of concrete," Advances in Concrete Construction, 1(2), 187-200, 2013.

[41] Türkiye Building Earthquake Code, (in Turkish), Ministry of Public Works and Settlement, 2018.

[42] R. Malm, "Predicting Shear Type Cracks Initiation and Growth in Concrete with Nonlinear Finite Elements Methods", PhD thesis, Royal Institute of Technology, Division of Structural Design and Bridges, Stockholm, Sweden. 2009.

[43] C. A. Coronado, M. M. Lopez, "Sensitivity analysis of reinforced concrete beams strengthened with FRP laminates," Cement and Concrete Composites, 28(1), 102-114, 2006.